

Resonant bowtie aperture nano-antenna for the control of optical nanocavities resonance

Fadi I. Baida and Thierry Grosjean

Département d'Optique P.M. Duffieux,

Institut FEMTO-ST, UMR 6174 CNRS

*Université de Franche-Comté, 25030 Besançon Cedex, France**

Abstract

Scanning Near-field Optical Microscopy (SNOM) has been successful in finely tuning the optical properties of photonic crystal (PC) nanocavities. The SNOM nanoprobe proposed so far allowed for either redshifting or blueshifting the resonance peak of the PC structures. In this Letter, we theoretically demonstrate the possibility of redshifting (up to +0.65 nm) and blueshifting (up to -5 nm) PC cavity resonance with a single SNOM probe. This probe is obtained by opening a bowtie-aperture nano-antenna (BNA) at the apex of a metal-coated tip. This double-way PC tunability is the result of a competition between the effects of the BNA resonance (induced electric dipole leading to a redshift) and the metal-coated tip (induced magnetic dipole giving rise to a blueshift) onto the PC mode volume. The sign of the spectral shift is modified by simply controlling the tip-to-PC distance. This study opens the way to the full postproduction control of the resonance wavelength of high quality factor optical cavities.

*Electronic address: fadi.baida@femto-st.fr

I. INTRODUCTION

It is well known that for a given optical cavity, the resonance properties depend on the volume allocated to the excited mode. This property generated several recent studies that deal with the resonance wavelength (RW) control especially in the case of high quality-factor resonators such as photonic crystal cavities. Modifications of this volume can be achieved through different physical processes. Thus, optical [1, 2], electrical [3, 4], chemical [5, 6] or mechanical [7, 8] effects were exploited to shift the RW by slightly modifying the cavity resonance properties. Plasmonic [9] and, more widely, any Fano-type resonances are also ideal candidates for such control.

In all cases, the perturbation must be small enough not to cancel the cavity resonance. Basically, the cavity mode volume can be modified by immersing a small dielectric element within the evanescent field of the cavity [10–14]. Thereby, the effective volume of the latter is increased (light penetrates inside the dielectric) leading to a red shift of its RW. Contrarily, if we replace dielectric by metal that inhibits the light permeation, the electromagnetic field will be mostly squeezed so that the whole mode volume decreases. The direct consequence is then a blue shift of the RW [2, 15]. Nonetheless, if the metallic structure exhibits localized resonance (almost with dipolar behavior), redshifts may occur after complete compensation of the mode squeezing due to the presence of the metal as already demonstrated in reference [9]. Generally, for these effects which are opposed, two cases are possible: either they are compensated, either one of them is dominant such that we can not discern them [17]. In all cases, the overall frequency shift is so small ($\Delta\lambda/\lambda \simeq 10^{-4}$) that resonators of very large Q-factors are needed [16] for experimental evidence. Thus, the question is how to control the contribution of each effect in order to actively control the RW? A basic idea consists of the design of an element that allows the two above cited effects and also permits adjusting the influence of each one through its interaction with the optical cavity. Nevertheless, the interaction of the cavity with this element should be as weak as possible to not completely break down the cavity resonance.

Appropriately, to highlight the existence of these two effects within a single configuration, some authors proposed a metal coated SNOM tip with small aperture at its apex in order to control the resonance wavelength of an optical cavity [17]. Such a perturbation element combines, at least, an induced electric dipole together with a magnetic one. Unfortunately,

the cavity-tip interaction was dominated by the magnetic contribution due to the large metal volume of the tip apex that is involved in the interaction. Nevertheless, theoretical calculations based on FDTD numerical simulations, showed that it is possible to get both red (very weak shift of only $30pm$) and blue shifts (almost 2.8\AA) with the same SNOM tip by placing its apex at specific positions in the vicinity of the cavity. By the way, the discrimination between the two effects is done spatially by exciting selectively the electric or the magnetic dipolar response of the tip through the knowledge of the electromagnetic field near the cavity.

As it is well-known, the magnetic effect, that is induced by the longitudinal component of the magnetic field (here along the tip axis) and leads to a blueshift, can be seen as a consequence of the cavity mode squeezing by the metallic apex of the tip. The electric effect of the tip apex is induced by the transversal component of the electric field around the tip apex and leads to a redshift of the resonance wavelength that can be seen to be due to an increase of the cavity mode volume. Based on Refs. [10, 17, 18], the contribution of the electric and magnetic dipoles to the wavelength shift can be written as:

$$\frac{\Delta\lambda}{\lambda} = \left[\frac{\Delta\lambda}{\lambda} \right]^e + \left[\frac{\Delta\lambda}{\lambda} \right]^m = (\alpha^e |E_{//}|^2 + \alpha^m |B_z|^2) \frac{e^{-2d/L_0}}{W_0} \quad (1)$$

Where α^e and α^m are electric and magnetic polarizabilities of the BNAT respectively, $E_{//}$ is the transverse component of the electric field within the unperturbed cavity, B_z is the magnetic longitudinal component at the top of the unperturbed cavity and W_0 is the total stored energy in the PC cavity at resonance. The decay term e^{-2d/L_0} is the same for both magnetic and electric field and allows the determination of the fields at the tip apex position (at a distance d from the cavity) through the knowledge of the decay length L_0 . The α^e and α^m terms have an opposite sign and both depend on the tip apex (the nature and the volume of metal that is involved by the tip-PC interaction for the magnetic term α^m and the size and shape of the aperture where the electric effect takes place for the electric term α^e). Consistently with the results of ref. [17] and with recent theoretical and experimental investigations [19, 20], a predominant contribution (from 2.5:1 to 10:1) of the magnetic effect was demonstrated compared to the electric one in the case of circular hole aperture engraved in metallic film.

In order to bypass this prevalence of the magnetic effect, a perturbation element that exhibits electric resonance would be necessary to reinforce the electric effect of the tip.

More precisely, this resonance must exhibit a small quality factor in order not to interact destructively with the optical cavity. Gap-based nano-antennas are ideal candidates due to their optical resonance that gives rise to spatially confined electric field over a broad spectral range (quality factor of around 3) [21].

In this paper, we propose an example of such configuration where an efficient resonator having quite large quality factor, a photonic crystal cavity, is coupled to a bowtie nano-aperture antenna (BNA) engraved at the end of a SNOM tip (called BNAT in the following). Due to the electric resonance of the BNA, the value of the ratio $\frac{\alpha^e}{W_0}$ is not only enhanced but it will depend on the distance between the tip and the cavity. In fact, when the BNA resonates, the interaction between the cavity and the BNAT can significantly decrease the stored energy (W_0) in the cavity due to a funneling effect [25] towards the BNA that dissipates a significant part of the energy by both scattering and absorption. In this case, the quasi-static approximation (a fortiori the depolarization regime [23]) is not fulfilled because the size of the BNAT apex cannot be considered larger than its skin depth at resonance due to the light funneling phenomenon toward the BNA. Analytic expression of α^e can then hardly be derived contrarily to the case of quasi-static (QS) approximation. In fact, as it will be demonstrated in the following, the QS approximation that leads to a constant value of α terms is only fulfilled when the BNA is off-resonance i.e. when the electric effect is canceled (only α^m is constant). Moreover, at the BNA resonance, the coupling between the two resonators greatly depends on the distance between them and thus the electromagnetic field above the PC does not undergo a basic evanescent decay as described in Eq. 1. Indeed, a critical coupling between the two resonators can take place for specific value of the BNA-to-PC distance [21, 24]. This sensitivity to the distance d , which will be presented in section III, is exploited to control the weight of the tip electric effect with respect to the magnetic one onto the PC cavity.

II. THE PROPOSED STRUCTURE

A. Study of the BNA

The BNA was designed through its geometrical parameters (see figure 1a) to obtain a resonance wavelength close to the one of the PC cavity. Thus, on the basis of ref. [22],

a metal coated SNOM tip with 100 nm thick aluminum layer and an apex radius R is considered to receive the BNA. The latter is supposed to be centered on the tip axis and has a gap of $g = 45$ nm and a side width of $D = 255$ nm (see figure 1a). The near-field spectral response of the tip, calculated by 3D-FDTD home-made code, is presented in figure 1b in addition to the spatial distribution of the electric field intensity in the yOz longitudinal plane at its resonance (inset of the same figure). The near-field spectrum given in figure 1b is calculated at 15 nm in front of the BNAT when it is illuminated by the fundamental guided mode of the optical fiber. Normalization of this near-field signal by the same intensity calculated without the BNA (uncoated tip) leads to an enhancement factor that reaches 280.

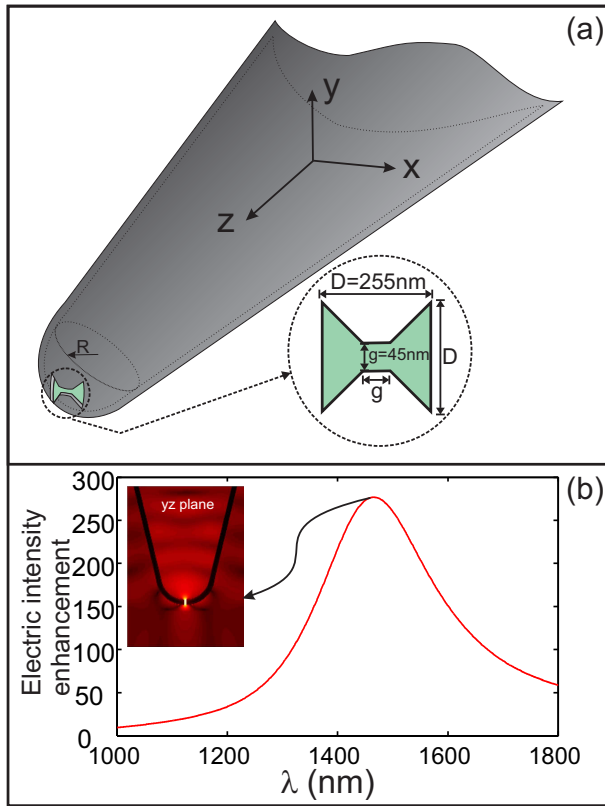


FIG. 1: (a) Schematic of the BNA engraved at the tip apex of radius R . (b) Enhancement factor of the BNAT measured 15 nm in front of its apex and defined as the ratio of the intensity with BNA by the same intensity calculated without metal coating. The inset of (b) shows the intensity distribution (logarithmic scale) in the yOz longitudinal plane to point out the light confinement occurring in the gap zone.

As clearly seen from the inset of figure 1b, the resonant BNA acts as a light concentrator. Note that this resonance is only obtained for the electric field component that is parallel to

the metallic arms of the BNA (Oy direction here). The resulting polarization sensitivity of the BNA allows distinction between the two transversal electric field components [22, 25] and will be used to discriminate between the magnetic effect of the electric one. Let us emphasize that this resonance corresponds to the excitation, at its cutoff wavelength, of the BNA fundamental guided mode that propagates through the metal thickness [26]. For a given metal, this cutoff wavelength can be analytically expressed as a function of the BNA geometrical parameters as demonstrated in ref. [26] allowing a very simple design of the BNA.

B. Study of the photonic crystal cavity

Let us now consider the photonic crystal -based optical cavity. It is composed of seven missed and aligned air holes in a triangular lattice photonic crystal that was designed to exhibit confined in-plane Bloch modes (period $a = 420 \text{ nm}$ and hole radius $r = 0.25a$)[27]. In addition, the two air holes located at the edges of the cavity are slightly moved out from the cavity in order to enhance the quality factor of its fundamental mode [28]. The PC is made in a InP layer of 300 nm thickness deposited on a $1 \mu\text{m}$ silica layer separating the InP from silicon substrate (see figure 2a). The fundamental mode of the cavity cannot be excited by propagating incident wave since it is spectrally located under the light line in the dispersion diagram of the PC structure.

Therefore, the excitation of the CL7 cavity is simulated with a 3D-FDTD homemade code by considering a point source (dipole) emitting over a wide spectral range and positioned in the vicinity of the cavity so that its orientation and position agree with the excitation of the cavity fundamental mode. The dipole source has a physical meaning since it can model a quantum emitter coupled to the cavity [29]. This coupling leads to the excitation of several cavity modes, thus, we have restricted our spectral study to a small spectral range centered on the resonance wavelength of the fundamental mode of the cavity. The near field spectral density of the CL7 cavity is shown on figure 2b with a RW equal to $\lambda_0^R = 1602.94 \text{ nm}$ and a quality factor estimated to $Q_{CL7} = 1590$.

3D-FDTD results giving the spatial distributions, at 15 nm above the PC cavity, of the transversal electric field components (E_x and E_y) are shown in figures 2c and d while the longitudinal magnetic field component (H_z) is given by the white contour plots on the same

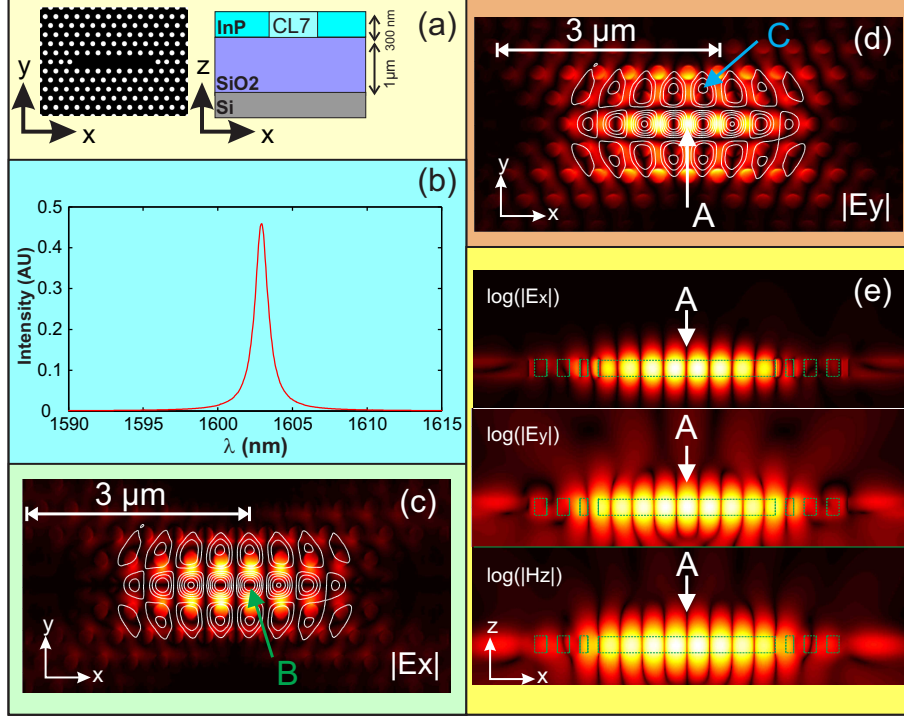


FIG. 2: Schematic of the proposed CL7 cavity in (a) with vertical and horizontal cross sections along the structure. The near-field spectrum, calculated at the center of the cavity, is presented in (b) where the resonance of the fundamental mode is shown to occur at $\lambda_0^R = 1602.94 \text{ nm}$ with a quality factor of $Q_{CL7} = 1590$. The amplitude of the two transversal electric field components at this resonance are given in the xOy plane located 15 nm above the InP membrane in (c) and (d). The white lines are iso-amplitude contours of the vertical component of the magnetic field (H_z) (e) Spatial distributions of the two transversal electric field and the longitudinal magnetic field components (logarithmic scale) at resonance in a vertical plane (xOz) passing by the center of the CL7.

figures. On the first hand, one can see from these two figures that the transversal (x and y) components are always spatially interleaved so that the E_x component vanishes when the E_y one is maximum. This specific property is of interest for the demonstration of the RW tunability in our case. In other words, when the BNA is placed above the center of the cavity (A position in figure 2c), its state (on- or off-resonance) can be simply controlled through its direction: on-resonance if the BNA's metallic arms are along the y -direction and off-resonance when they are along the x -direction, without changing the BNAT spatial position [25]. This allows here for differentiating the interaction effect induced by the BNA

resonance (dielectric term) from that of the tip metal coating (magnetic response). From figure 2e, that shows the spatial distribution of the two transverse electric field components and the longitudinal magnetic one in the xOz vertical plane, we estimated the value of the decay length to be $L_0 = 98 \text{ nm}$. We verified that, both electric and magnetic fields have the same decay length.

III. STUDY OF THE COUPLING

The whole structure (BNAT + CL7) is numerically studied with a 3D-FDTD homemade code that incorporates non-uniform mesh together with a sub-gridding technique in order to faithfully describe the structure. First, the BNAT is supposed to be centered on the CL7 cavity. According to figure 2c and d, only the E_y component of the electric field exists at this location (A), E_x is equal to zero. Consequently, the BNA metallic arms must be oriented along the y -direction to induce its resonance.

Optical near-field spectra calculated 15 nm above the CL7 are presented in figure 3a for different values of the BNAT-to-CL7 distance (d) when the BNA is oriented along the Oy direction (BNA on-resonance) and for a tip apex of $R = 250 \text{ nm}$. We recall that R is the dielectric tip apex radius before the metal coating). One can clearly see from figure 3a the occurrence of two opposite behaviors: a significant redshift for large value of d and a small blue one for $d = 30 \text{ nm}$. Thus, two different phenomena are in competition: the metallic tip effect or magnetic effect that squeezes the PC cavity mode (blue shift) and the BNA resonance that tends to increase the mode volume by extending light distribution inside its gap (dielectric resonance). This interpretation is clearly confirmed thanks to the results of figure 3b obtained for off-resonant BNA and showing, similarly to reference [15], only blue shifts whatever the distance separating the tip from the cavity. However, the quality factor of these resonances evolves differently depending on the BNA state (on or off) as it will be seen in the following.

Second, in order to quantify the magnetic and the electric effects, we have numerically studied the coupling for different values of the tip radius and for both on- and off-resonant BNA. Figure 4a shows the variations of the relative shift as a function of the BNAT-to-PC distance for off-resonant BNA when the tip is placed in the center of the CL7 cavity (point A indicated by the white arrow in figure 2d). Note that at this location, the longitudinal

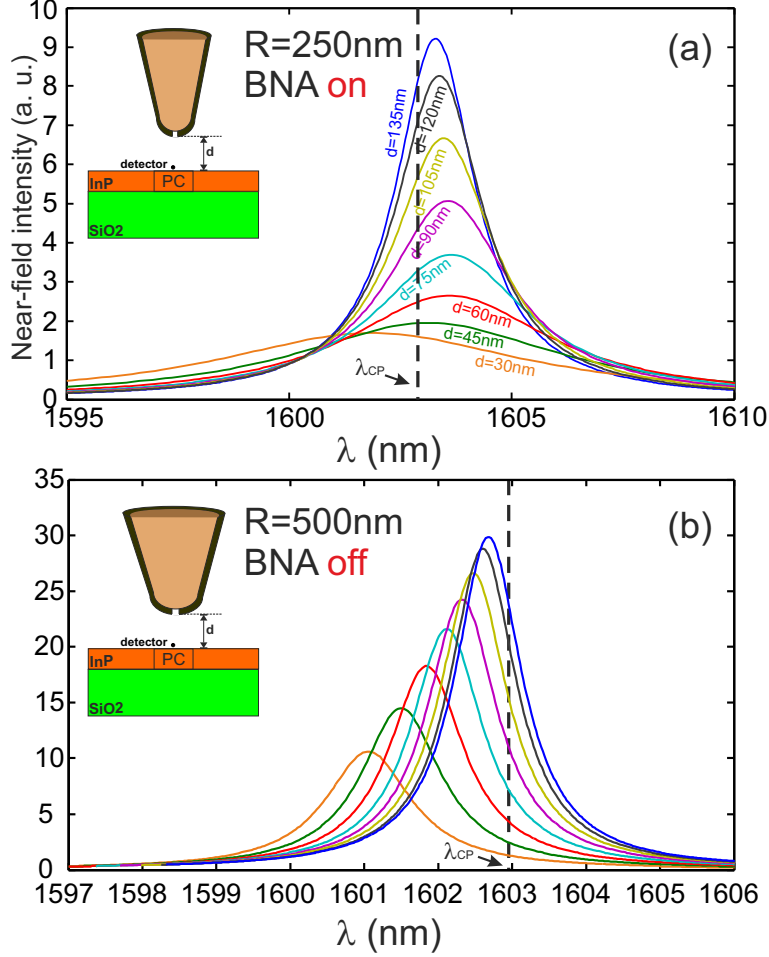


FIG. 3: Near field spectra calculated 15 *nm* in front of the PhC for two different BNAT. In (a) the BNA resonates meaning that its metallic arms are along the *y*-direction. In addition, the tip radius is fixed to $R = 250 \text{ nm}$ in order to minimize the blue shift that directly depends on the tip size. Consequently, blueshift only appears for a small distance $d = 30 \text{ nm}$ while the BNA resonance is responsible for the redshift because a part of the light penetrates inside the gap leading to a larger mode volume. In (b) the radius of the tip is increased to $R = 500 \text{ nm}$ to enhance the mode squeezing and the BNA is rotated by 90° in order to inhibit its resonance. In this case, the BNAT almost plays the role of a metallic rod as in ref. [2] leading only to a blueshift whatever the value of the distance d is as experimentally demonstrated in [15].

magnetic field vanishes (see white contours) and the obtained magnetic effect is due to the interaction of the tip sidewalls with the closest lobes of the magnetic field. In this case, the electric term of Eq. 1 is negligible and only magnetic coupling occurs between the BNAT and the PC (second term of Eq. 1). The linear behaviors observed in figure 4a confirm that

the magnetic effect can be derived from a quasi-static (QS) approximation as in Ref. [17] whatever the value of the tip apex radius (from $R = 180nm$ to $R = 500nm$).

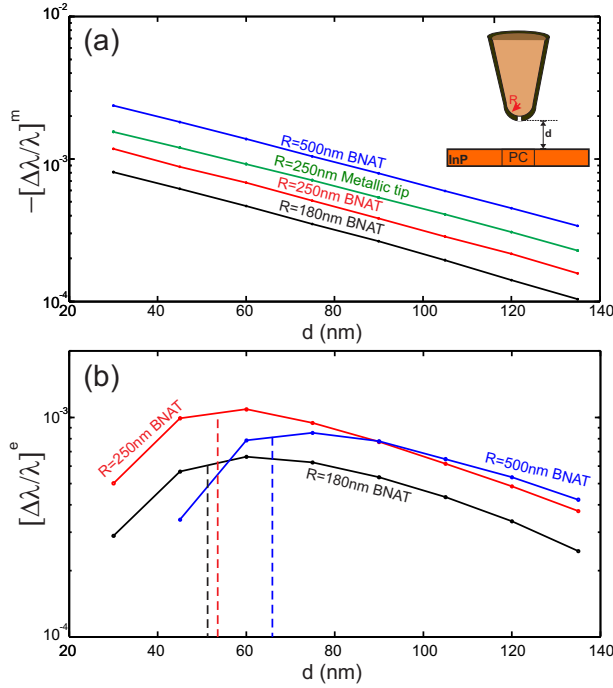


FIG. 4: Magnetic in (a) and electric in (b) relative shifts of the resonance wavelength of the CL7 fundamental mode as a function of the BNAT-to-CL7 distance d . Three different BNAT apex radius are considered ($R = 180nm$ in black, $R = 250nm$ in red and $R = 500nm$ in blue). The magnetic shift induced by an apertureless SNOM tip with radius $R = 250nm$ is also presented in green line in (a).

On the other hand, the slope of the four lines in figure 4a, which is equal to $\frac{-2}{L_0}$ is in a excellent agreement with the decay length $L_0 = 98nm$ of the electromagnetic field above the unperturbed cavity. Values of $L_0 = 108nm$, $105nm$, $104nm$ and $102nm$ are obtained for $R = 500nm$, $250nm$, $300nm$ and $180nm$ respectively. Once again, the QS approximation is validated in the case of passive BNAT (off-resonant BNA). Nevertheless, the small increasing in the decay length with respect to the tip radius can be seen as a slight increasing of the longitudinal component of the magnetic field (B_z) with respect to the unperturbed cavity due to the coupling with the BNAT. Nonetheless, we have calculated the cavity energy W_0 and determine the effective magnetic polarizability, for the four values of the radius, through Eq. 1. The obtained values are : $\alpha_{R=180nm}^m = -8.53 \times 10^{-21}m^3/\mu_0$, $\alpha_{R=250nm}^m = -12.53 \times 10^{-21}m^3/\mu_0$, $\alpha_{R=300nm}^m = -15.37 \times 10^{-21}m^3/\mu_0$ and $\alpha_{R=500nm}^m = -25.96 \times 10^{-21}m^3/\mu_0$.

These values well agree with the value ($\alpha_{R=200nm}^m = -12 \times 10^{-21} m^3/\mu_0$) obtained in ref. [17] for a cylindrical aperture metal coated SNOM tip with a radius of $200nm$. Note that the magnetic polarizability is directly linked to the metal volume that is involved in the interaction so that the presence of the aperture will slightly decrease its value. We have verified this assumption through the determination of the polarizability of an apertureless metallic tip with radius $R = 250nm$ and get a value of $\alpha^m = -17.44 \times 10^{-21} m^3/\mu_0$ instead of $\alpha_{R=250nm}^m = -12.53 \times 10^{-21} m^3/\mu_0$ with BNA. By the way, we stress the fact that apertures in SNOM tip are not necessary to induce the magnetic effect; simple metallic nano-rod is more efficient as already demonstrated in ref. [2]. The electric term of Eq. 1 can be determined by subtracting the pure magnetic effect of figure 4a, observed in the case of off-resonant BNA, from the effect corresponding to a resonantly excited BNA (keeping the tip at the same position and rotating the BNA by 90°). The obtained values are presented in figure 4b. Contrarily to the magnetic term, the relative shift (in logarithmic scale) of the induced electric dipole exhibits a non-linear behavior versus the BNAT-to-PC distance clearly denoting the non validity of the quasi-static approximation. A maximum of red-shift is obtained (see vertical dashed lines in figure 4b) corresponding to a critical coupling between the two resonators (i.e. maximum energy transfer between them) [24]. As expected, this critical tip-to-PC distance increases with the tip apex radius due to the redistribution of the electromagnetic energy inside and around the cavity [30].

Other simulations were done for different configurations including both the modification of the tip position, the BNA direction (on- and off-resonance) and the tip apex radius. These configurations are compared to the case of an uncoated dielectric tip (DT) and to the case of a metallic tip (MT). The numerical results are presented in figure 5. Because negative and positive shifts occur, we plotted here the RW values (figure 5a-c) instead of the relative shift as in figure 4. The Q-factor variations are also given in figure 5d. As expected, figure 5a shows the competition effect between the induced electric and the magnetic dipoles at the tip apex. This competition only appears when the BNA resonates (position A given by white arrow on figure 2d) i.e. when the antenna gap is immersed in a transverse electric field directed along its metallic arm (y-direction here). If the BNA position corresponds to a node of transverse electric field (positions B or C pointed by the green and the blue arrows respectively) or if it is off-resonance (even in the position A), only resonance blueshifts occur. In addition, for BNAT with large apex radius, the blue shift is more pronounced meaning

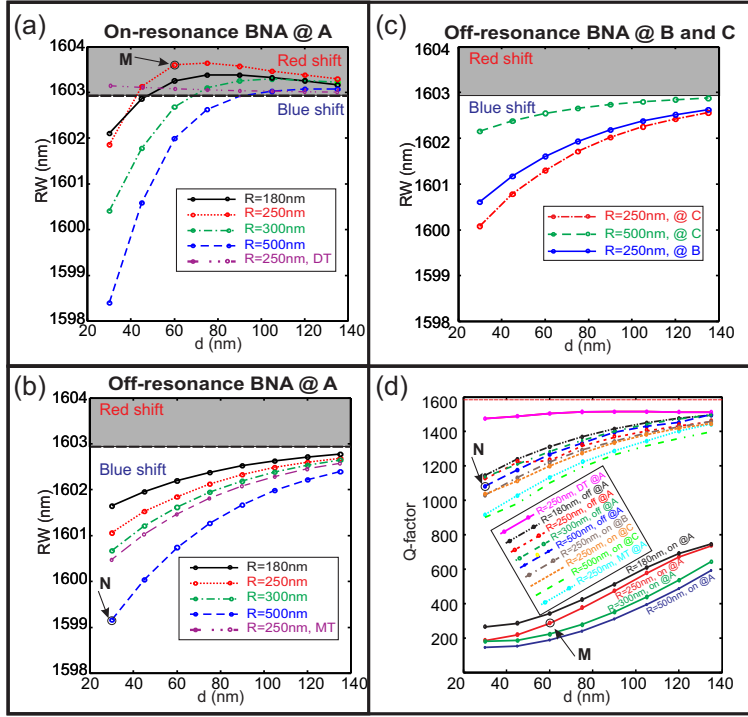


FIG. 5: (a) Resonance wavelengths (RW) calculated in the case of a resonant BNAT placed above the CL7 center in position A (see white arrow in figure 2d) as a function of the tip-to-CL7 tip distance d . The RW shift is both positive and negative with respect to d demonstrating the double-way tunability. The case of a pure dielectric tip (similar to that of ref. [17]) is also presented in dashed-dotted-dotted magenta line. (b) same as (a) in the case of non-resonant BNAT. Electric effect is very weak and only blue shifts are obtained. The case of a pure metallic tip (as in ref. [2]) is presented for comparison. (c) Same as (a) and (b) but for BNAT apex positioned at the vertical of B and C positions (see figures 2c and d). (d) Q-factors of the thirteen studied configurations corresponding to different apex radii (from $R = 180nm$ to $R = 500nm$) and BNA state (on or off resonance) including uncoated dielectric tip (DT) and metallic tip (MT) as a function of the BNAT-to-CL7 distance d . The red dashed horizontal lines at the top of the figure corresponds to the case of the unperturbed CL7 cavity ($Q_{CL7} = 1590$).

larger magnetic polarizability of the tip apex as already demonstrated above. Meanwhile, the quality factor given in figure 5d is significantly reduced when the BNA resonates because the stored electromagnetic energy that was confined in the CL7 cavity is now dissipated by the BNA. This leads to a decrease of the photon lifetime and thus to a decrease of the

Q-factor of the cavity resonance. Similar decreasing of Q-factor was also obtained in refs. [10, 18] even if no electric resonance is excited (passive dielectric tip).

Note that, on one hand, for a big tip with $R = 500 \text{ nm}$ (blue dashed line in figure 5a), the two effects (blue and red shifts) compensate for a distance $d = 90 \text{ nm}$ while this occurs at smaller distance ($d \simeq 40 \text{ nm}$) for a tip apex radius of $R = 250 \text{ nm}$ (red dotted line in figure 5a). Nevertheless, for both configurations, the quality factor of the whole structure decreases to $Q_{90}^{500} = 310$ and $Q_{40}^{250} = 210$ respectively instead of $Q_{CL7} = 1590$ for the unperturbed cavity (see figure 5d). Consequently, from ref. [25], we estimate that the energy dissipated by the BNAT (radiated inside the fiber and/or absorbed by the metal) is around 80% and 86% of the total energy initially stored in the cavity respectively. On the other hand, for $R = 500 \text{ nm}$, a $\Delta\lambda = 5 \text{ nm}$ blueshift is achieved by only approaching the BNAT at 30 nm from the PC. Larger shifts can occur for smaller tip-to-PC distances as already experimentally demonstrated in ref. [15] where 16nm blueshift were observed for $d = 10\text{nm}$. This value corresponds to an efficient tunability of the cavity resonance in comparison with the value of $\Delta\lambda = 1.7 \text{ nm}$ that was recently obtained by focusing effect on plasmonic nanorod coupled with a PC cavity [2].

Finally, the light distribution inside the structure is shown in fig. 6 at the resonance wavelength of the hybrid structure for two contrasting configurations indicated by the points M and N in figure 5d. Our main goal is to point out the spatial expansion or squeezing of the mode with regard to the case of the unperturbed cavity resonance given in figure 6c. As it can be seen on figure 6a, the resonance of the BNA leads to a dramatic reduction of the light energy inside the CL7 due to a significant penetration inside the gap zone (compared to the figure 6c). On the contrary, a volume reduction of the energy distribution occurs (see figure 6b) near the BNAT accompanied with a small decrease of the photon lifetime in the CL7 cavity (slight reduction of the resonance quality factor) when the BNA is off-resonant.

This study clearly demonstrated that a BNAT tip has the ability of red- and blue-shifting the resonance of an optical nanocavity in a fine and reversible post-production tuning. Nevertheless, as in ref. [10], redshifts are achieved at the cost of significant Q-factor reduction. An experimental demonstration of the coupling between the same PC cavity (CL7) and a BNAT was already performed [25] but only blueshift of the cavity resonance was observed because the nano-antenna effect was not as strong as predicted. This points out that the tip design is critical in the achievement of the desired effect onto the nanocavity. Based on

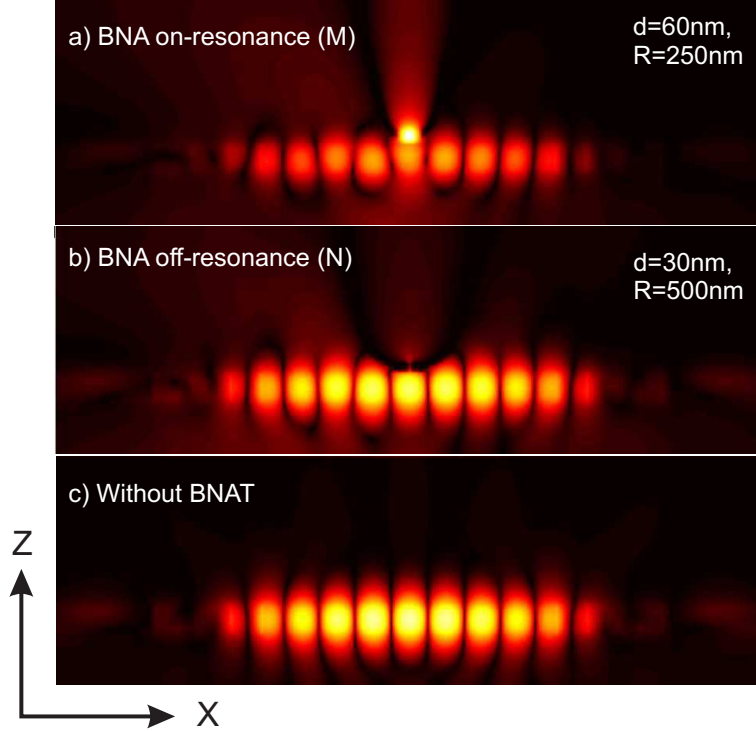


FIG. 6: (a-c) calculated electric intensity distributions (in logarithmic scale) corresponding to the case of the two points M (in figure 5a and d) and N (in figure 5b and d) in addition to the case of the unperturbed PhC respectively. One can clearly see in (a) that the BNA pumps the PhC energy and then dissipates it mainly inside the tip while the spatial extension of the cavity mode is clearly reduced in (b), compared to the unperturbed cavity in (c), due to the presence of the metal tip apex that squeezes the electromagnetic evanescent field down to the cavity. This result is consistent with the obtained discrepancy between the Q-factor of these two configurations given in figure 5b

this configuration, alternative tip and antenna geometries may be found to accomplish this two-way spectral tunability of a nanocavity resonance while preserving its Q-factor even in the case of redshift by inhibiting the far-field scattering toward the antenna.

Acknowledgements: The authors are indebted to Prof. K. Kuipers for helpful discussions and to Dr. M. Dankar for her technical advise. This work is funded by “Agence Nationale de la Recherche” under contract number ANR10-NANO-002, the program “BQR PRES Bourgogne Franche-Comté”. It is supported by the “Pôle de compétitivité Microtechnique”, the “Labex ACTION” program (Contract ANR-11-LABX-01-01) and the “Mésocentre” of the University of Franche-Comté.

-
- [1] M. Belotti, J. F. G. Lopez, S. D. Angelis, M. Galli, I. Maksymov, L. C. Andreani, D. Peyrade, and Y. Chen, "All-optical switching in 2D silicon photonic crystals with low loss waveguides and optical cavities" *Opt. Express* **16**, 11624 (2008).
- [2] I. S. Maksymov and A. E. Miroshnichenko, "Active control over nanofocusing with nanorod plasmonic antennas" *Opt. Express* **19**, 5888 (2011).
- [3] I. Fushman, E. Waks, D. Englund, N. Stoltz, P. Petroff, and J. Vuckovic, "Ultrafast nonlinear optical tuning of photonic crystal cavities" *Appl. Phys. Lett.* **90**, 091118 (2007).
- [4] A. Majumdar, J. Kim, J. Vuckovic, and F. Wang, "Electrical control of silicon photonic crystal cavity by graphene" *Nano Lett.* **13**, 515–518 (2013).
- [5] P. El-Kallassi, R. Ferrini, L. Zuppiroli, N. Le Tomas, R. Houdré, A. Berrier, S. Anand, and A. Talneau, "Optical tuning of planar photonic crystals infiltrated with organic molecules" *J. Opt. Soc. Am. B* **24**, 2165–2171 (2007).
- [6] T. Cai, R. Bose, G. S. Solomon, and E. Waks, "Controlled coupling of photonic crystal cavities using photochromic tuning" *Appl. Phys. Lett.* **102**, 141118 (2013).
- [7] S. Vignolini, F. Riboli, D. S. Wiersma, L. Balet, L. H. Li, M. Francardi, A. Gerardino, A. Fiore, M. Gurioli, and F. Intonti, "Nanofluidic control of coupled photonic crystal resonators" *Appl. Phys. Lett.* **96**, 141114 (2010).
- [8] N. Descharmes, U. Dharanipathy, Z. Diao, M. Tonin, and R. Houdré, "Observation of back-action and self-induced trapping in a planar hollow photonic crystal cavity" *Phys. Rev. Lett.* **110**, 123601 (2013).
- [9] M. Barth, S. Schietinger, S. Fischer, J. Becker, N. Nüsse, T. Aichele, B. Löchel, C. Sönnichsen, and O. Benson, "Nanoassembled plasmonic-photonic hybrid cavity for tailored light-matter coupling" *Nano Lett.* **10**, 891–895 (2010).
- [10] A. F. Koenderink, M. Kafesaki, B. C. Buchler, and V. Sandoghdar, "Controlling the resonance of a photonic crystal microcavity by a near-field probe" *Phys. Rev. Lett.* **95**, 153904 (2005).
- [11] I. Marki, M. Salt, and H. P. Herzig, "Tuning the resonance of a photonic crystal microcavity with an AFM probe" *Opt. Express* **14**, 2969 (2006).
- [12] W. C. L. Hopman, A. J. F. Hollink, R. M. de Ridder, K. O. van der Werf, V. Subramaniam, and W. Bogaerts, "Nano-mechanical tuning and imaging of a photonic crystal micro-cavity

- resonance" *Opt. Express* **14**, 8745 (2006).
- [13] L. Lalouat, B. Cluzel, P. Velha, E. Picard, D. Peyrade, J. P. Hugonin, P. Lalanne, E. Hadji, and F. de Fornel, "Near-field interactions between a subwavelength tip and a small-volume photonic-crystal nanocavity" *Phys. Rev. B* **76**, 041102 (2007).
- [14] G. L. Gac, A. Rahmani, C. Seassal, E. Picard, E. Hadji, and S. Callard, "Tuning of an active photonic crystal cavity by an hybrid silica/silicon near-field probe" *Opt. Express* **17**, 21672 (2009).
- [15] T. Grosjean, A. E. Eter, M. Mivelle, T.-P. Vo, A. Belkhir, C. Ecoffey, G. L. Gac, D. Nedeljkovic, A. Rahmani, C. Seassal, S. Callard, and F. Baida, "Extraordinary blueshift of a photonic crystal nanocavity by reducing its mode volume with an opaque microtip" *Appl. Phys. Lett.* **101**, 051102 (2012).
- [16] S. Mujumdar, A. F. Koenderink, T. Sunner, B. C. Buchler, M. Kamp, A. Forchel, and V. Sandoghdar, "Near-field imaging and frequency tuning of a high-Q photonic crystal membrane microcavity" *Opt. Express* **15**, 17214–17220 (2007).
- [17] M. Burrese, T. Kampfrath, D. van Oosten, J. C. Prangma, B. S. Song, S. Noda and L. Kuipers, "Magnetic Light-Matter Interactions in a Photonic Crystal Nanocavity" *Phys. Rev. Lett.* **105**, 123901 (2010).
- [18] S. Vignolini, F. Intonti, F. Riboli, L. Balet, L. H. Li, M. Francardi, A. Gerardino, A. Fiore, D. S. Wiersma, and M. Gurioli, "Magnetic Imaging in Photonic Crystal Microcavities" *Phys. Rev. Lett.* **105**, 123902 (2010).
- [19] N. Rotenberg, M. Spasenovic, T. L. Krijger, B. le Feber, F. J. García de Abajo, and L. Kuipers, "Plasmon Scattering from Single Subwavelength Holes" *Phys. Rev. Lett.* **108**, 127402 (2012).
- [20] N. Rotenberg, T. L. Krijger, B. le Feber, M. Spasenović, F. Javier García de Abajo, and L. Kuipers "Magnetic and electric response of single subwavelength holes" *Phys. Rev. B* **88**, 241408 (2013).
- [21] A. El Eter, T. Grosjean, P. Viktorovitch, X. Letartre, T. Benyattou, and F. I. Baida "Huge light-enhancement by coupling a bowtie nano-antenna's plasmonic resonance to a photonic crystal mode" *Opt. Express* **22**, 14464–14472 (2014).
- [22] M. Mivelle, I. A. Ibrahim, F. Baida, G. W. Burr, D. Nedeljkovic, D. Charraut, J.-Y. Rauch, R. Salut, and T. Grosjean, "Bowtie nano-aperture as interface between near-fields and a single-mode fiber" *Opt. Express* **18**, 15964–15974 (2010).

- [23] R. Inoue, H. Kitano, and A. Maeda, "Double-sphere model in the enclosed cavity perturbation technique" *J. Appl. Phys.* **93**, 2736–2745 (2003).
- [24] A. Belarouci, T. Benyattou, X. Letartre, and P. Viktorovitch, "3D light harnessing based on coupling engineering between 1D-2D Photonic Crystal membranes and metallic nano-antenna" *Opt. Express* **18**, 381–394 (2010).
- [25] M. Mivelle, P. Viktorovitch, F. I. Baida, A. E. Eter, Z. Xie, T.-P. Vo, E. Atie, G. W. Burr, D. Nedeljkovic, J.-Y. Rauch, S. Callard, and T. Grosjean, "Light funneling from a photonic crystal laser cavity to a nano-antenna: overcoming the diffraction limit in optical energy transfer down to the nanoscale" *Opt. Express* **22**, 15075–15087 (2014).
- [26] I. A. Ibrahim, M. Mivelle, T. Grosjean, J. T. Allegre, G. W. Burr, and F. I. Baida, "Bowtie-shaped nanoaperture: a modal study" *Opt. Lett.* **35**, 2448–2450 (2010).
- [27] C. Monat, C. Seassal, X. Letartre, P. Regreny, M. Gendry, P. R. Romeo, P. Viktorovitch, M. L. V. d'Yerville, D. Cassagne, J. P. Albert, E. Jalaguier, S. Pocas, and B. Aspar, "Two-dimensional hexagonal-shaped microcavities formed in a two-dimensional photonic crystal on an InP membrane" *J. Appl. Phys.* **93**, 23–31 (2003).
- [28] Y. Akahane, T. Asano, B.-S. Song, and S. Noda, "High-Q photonic nanocavity in a two-dimensional photonic crystal" *Nature* **425**, 944–947 (2003).
- [29] L. Novotny and B. Hecht, *Principles of Nano-Optics* (Cambridge University Press, 2006).
- [30] B. le Feber, N. Rotenberg, D. M. Beggs, and L. Kuipers, "Simultaneous measurement of nanoscale electric and magnetic optical fields" *Nature Photon.* **8**, 43–46 (2014).